DOI 10.1007/s11595-016-1350-7

Formation and Mechanical Properties of Zr-Nb-Cu-Ni-Al-Lu Bulk Glassy Alloys with Superior Glass-Forming Ability

ZHAO Xiangjin[1], LIU Wei[1], LIU Li[1], ZHANG Tao[2], PANG Shujie[2], MA Chaoli[2]

(1. School of Environment and Materials Engineering, Yantai University, Yantai 264005, China; 2. Department of Materials Science and Engineering, Beijing University of Aeronautics and Astronautics, Beijing 100083, China)

Abstract: Glass-forming ability (GFA) and mechanical properties of $(Zr_{0.58}Nb_{0.03}Cu_{0.16}Ni_{0.13}Al_{0.10})_{100-x}Lu_x$ (x = 0-3 at%) alloys have been investigated. The GFA of $Zr_{58}Nb_3Cu_{16}Ni_{13}Al_{10}$ alloy is dramatically enhanced by adding Lu. The $(Zr_{0.58}Nb_{0.03}Cu_{0.16}Ni_{0.13}Al_{0.10})_{98}Lu_2$ alloy possesses the highest GFA in the studied Zr-Nb-Cu-Ni-Al-Lu alloys, with its critical diameter for glass formation reaching 20 mm by copper-mould casting method, while that of the Lu-free $Zr_{58}Nb_3Cu_{16}Ni_{13}Al_{10}$ alloy is 7 mm. The critical diameters of $(Zr_{0.58}Nb_{0.03}Cu_{0.16}Ni_{0.13}Al_{0.10})_{100-x}Lu_x$ (x = 1 at% and 3 at%) alloys are 15 mm and 12 mm, respectively. The Lu addition to $Zr_{58}Nb_3Cu_{16}Ni_{13}Al_{10}$ alloy induces the change of initial crystallization phases from face-centred-cubic Zr_2Ni and tetragonal Zr_2Ni phases for the Lu-free $Zr_{58}Nb_3Cu_{16}Ni_{13}Al_{10}$ alloy to an icosahedral quasi-crystalline phase for the Lu-doped alloys, which may be the origin for the enhanced GFA of the Lu-doped alloys. The compressive fracture strength and plastic strain of the bulk glassy $(Zr_{0.58}Nb_{0.03}Cu_{0.16}Ni_{0.13}Al_{0.10})_{98}Lu_2$ alloy are 1 610 MPa and 1.5%, respectively.

Key words: metallic glass; zirconium-based alloy; glass-forming ability; mechanical properties

1 Introduction

Over the last several decades, multi-component bulk metallic glasses (BMGs) have attracted great interest due to their unique physical, mechanical and chemical properties[1-3], and many kinds of BMGs have been developed including Mg-, Ln-, Cu-, Fe-, Pd- and Zr-based systems. It is well known that Zr-based BMGs have high glass-forming ability (GFA) and thermal stability, excellent strength, as well as good wear and corrosion resistance[4-7]. These alloys have received increasing attention in both the basic science and potential for engineering applications as structural metallic materials[8]. So far, several Zr-based metallic alloys with high GFA, such as Zr-Al-TM (TM = Co, Ni, Cu)[4], Zr-Al-Ni-Cu[9], Zr-Ti-Ni-Cu-Be[5], Zr-M-Cu-Ni-Al (M = Ti, Nb) [10, 11], Zr-Al-Cu-Ag[12] and Zr-Al-Co-Ag[13] alloys, have been developed. The Zr–Nb–Cu–Ni–Al system is a well studied metallic glass owing to its high GFA, and the measured critical cooling rate for glass formation is less than 10 K s^{-1}[10]. We have reported that minor addition of Y to $Zr_{58}Nb_3Cu_{16}Ni_{13}Al_{10}$ alloy not only induced an icosahedral quasi-crystalline phase (I-phase) formation but also greatly enhanced the GFA[14]. Recently, based on the study on the effect of Lu on the glass formation, $(Zr_{0.58}Nb_{0.03}Cu_{0.16}Ni_{0.13}Al_{0.10})_{98}Lu_2$ alloy with unusually high GFA has been developed, and it can be cast fully into BMG with a diameter of 20 mm by copper-mould casting.

Consequently, we focus on the glass formation, thermal stability and mechanical properties of $(Zr_{0.58}Nb_{0.03}Cu_{0.16}Ni_{0.13}Al_{0.10})_{100-x}Lu_x$ (x = 0, 1, 2 and 3 at%) alloys. For understanding the effect of Lu element on the GFA of Zr-Nb-Cu-Ni-Al-Lu alloys, the crystallization behaviors of the Lu-free and Lu-doped alloys are studied. Mechanical properties of these BMGs are also examined.

2 Experimental

Alloy ingots with nominal compositions of $(Zr_{0.58}$

(Received: Oct. 25, 2014; Accepted: Nov. 26, 2015)

ZHAO Xiangjin(赵相金): Assoc. Prof.; Ph D; E-mail: zl2915@ytu.edu.cn

Funded by the National Natural Science Foundation of China (Nos. 51101133, 51101134), the Encouraging Foundation for Outstanding Youth Scientists of Shandong Province, China (No. BS2012CL036) and the Natural Science Foundation of Shandong Province, China (No. ZR2011EL025)

$Nb_{0.03}Cu_{0.16}Ni_{0.13}Al_{0.10})_{100-x}Lu_x$ (x = 0 at%, 1 at%, 2 at% and 3 at%) were prepared by arc-melting a mixture of the pure metals Zr, Nb, Cu, Ni, Al and Lu in a Ti-gettered argon atmosphere. From the master alloys, ribbons were prepared by single-roller melt-spinning technique in an argon atmosphere. For the smaller rod-shaped sample (≤ 10 mm in diameter), the ingot was remelted in a quartz tube using an induction heating coil in an argon atmosphere, and then injected into a copper mold through a nozzle. For the larger rod-shaped sample (≥12 mm in diameter), the ingot was remelted in a quartz cup using a tilting induction furnace, and the molten alloy was poured into a copper mold in an argon atmosphere. The structure of cross sections of as-cast rods was characterized by X-ray diffraction (XRD) using a Bruker AXS D8 X-ray diffractometer with Cu-Kα radiation. The glass transition temperature (T_g), onset temperature of crystallization (T_x), onset melting temperature (T_m) and offset melting temperature (T_l) were measured by a NETZSCH DSC 404 C differential scanning calorimeter (DSC) at a heating rate of 0.33 K s^{-1} under a flowing purified argon atmosphere. To study the crystallization behavior, the glassy ribbons were annealed to crystallization in the DSC cell at a heating rate of 0.33 K s^{-1}, and then cooled to room temperature. The crystallized phase structure was identified by XRD and a JEM2100F transmission electron microscopy (TEM), operated at the acceleration voltage of 200 kV. The samples for TEM were the ribbons thinned electrochemically by jet polishing at 263 K and 20 V, using a solution of CH_3OH and HNO_3 in a volume ratio of 2:1. Mechanical properties under uniaxial compression were examined with a SANS CMT5504 testing machine at a strain rate of 4.17×10^{-4} s^{-1} in ambient atmosphere. The sample dimension for the compression test was 2 mm in diameter and 4 mm in height. The fracture surface was observed by JSM-5800 scanning electron microscopy (SEM).

3 Results and discussion

For investigating the effect of the addition of Lu element on the GFA, rod samples of Zr-Nb-Cu-Ni-Al-Lu alloys with different diameters were fabricated. Fig. 1 shows the XRD patterns of the $(Zr_{0.58}Nb_{0.03}Cu_{0.16}Ni_{0.13}Al_{0.10})_{100-x}Lu_x$ (x = 0 at%, 1 at%, 2 at% and 3 at%) cast rods with critical diameters (dmax) for glass formation. All the XRD patterns exhibit a principal halo and no sharp diffraction peaks corresponding to a crystalline phase, indicating their glassy nature within the detection limit of XRD.

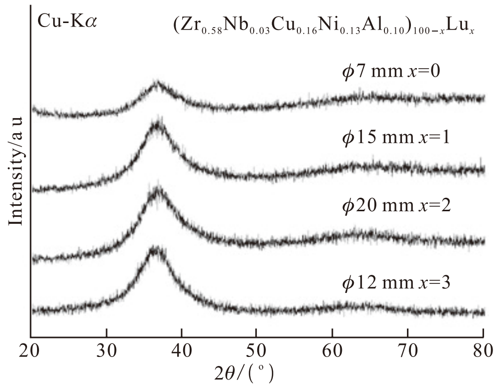

Fig.1 X-ray diffraction patterns of $(Zr_{0.58}Nb_{0.03}Cu_{0.16}Ni_{0.13}Al_{0.10})_{100-x}Lu_x$ (x = 0-3 at%) cast rods with their critical diameters for glass formation

The critical diameters of the studied alloys are summarized in Table 1. It is found that the GFA of $(Zr_{0.58}Nb_{0.03}Cu_{0.16}Ni_{0.13}Al_{0.10})_{100-x}Lu_x$ (x = 0 at%, 1 at%, 2 at% and 3 at%) alloys is very sensitive to the content of Lu and the Lu-doped alloys have higher GFA than the Lu-free alloy. The $(Zr_{0.58}Nb_{0.03}Cu_{0.16}Ni_{0.13}Al_{0.10})_{98}Lu_2$ alloy possesses the highest GFA in the studied alloy system, and its critical diameter for glass formation reaches as high as 20 mm. The critical diameter of the $(Zr_{0.58}Nb_{0.03}Cu_{0.16}Ni_{0.13}Al_{0.10})_{100-x}Lu_x$ (x = 1 at% and 3 at%) is 15 and 12 mm, respectively. In comparison, the maximum diameter for glass formation is only 7 mm for the Lu-free $Zr_{58}Nb_3Cu_{16}Ni_{13}Al_{10}$ alloy under the same experimental conditions.

The effect of lutetium on the thermal properties of the $Zr_{58}Nb_3Cu_{16}Ni_{13}Al_{10}$ alloy was investigated by DSC. Fig. 2 shows the DSC curves of melt-spun $(Zr_{0.58}Nb_{0.03}Cu_{0.16}Ni_{0.13}Al_{0.10})_{100-x}Lu_x$ (x = 0 at%, 1 at%, 2 at% and 3 at%) glassy ribbons. As shown in Fig.2, with increasing temperature, all the alloys exhibit distinct glass transition, followed by the appearance

Table 1 Some thermal parameters and critical diameters of $(Zr_{0.58}Nb_{0.03}Cu_{0.16}Ni_{0.13}Al_{0.10})_{100-x}Lu_x$ (x = 0-3 at%) glassy alloys

Lu content/at%	d_{max}/mm	T_g/K	T_x/K	T_m/K	T_l/K	ΔT_x/K	T_g/T_l	$T_x/(T_g+T_l)$
0	7	667	759	1 054	1 160	92	0.575	0.415
1	15	662	748	1 077	1 159	86	0.571	0.411
2	20	662	741	1 075	1 171	79	0.565	0.404
3	12	657	748	1 076	1 180	91	0.557	0.407

of a wide supercooled liquid region, crystallization and then melting behaviors. The thermal parameters of T_g, T_x, T_l and T_m, derived from the DSC curves, are summarized in Table 1. It is evident that the addition of Lu affects the thermal stability of $Zr_{58}Nb_3Cu_{16}Ni_{13}Al_{10}$ glassy alloy. The Lu addition results in a decrease in T_g and T_x and an increase in T_m and T_l, while no obvious change in T_l is observed with the introduction of 1 at% Lu. The values of some GFA indicators, including the supercooled liquid region ΔT_x ($\Delta T_x = T_x - T_g$), the reduced glass transition temperature T_{rg} ($T_{rg} = T_g/T_l$) and γ [$\gamma = T_x/(T_g + T_l)$][15] for the present glassyalloys are also shown in Table 1. With the Lu content increasing from 0 to 2 at%, the ΔT_x value decreases from 92 to 79 K, then increases slightly and reaches the maximum value of 91 K at 3 at% Lu. The decrease in T_{rg} and γ are also observed for the Lu-doped alloys. It can be concluded that the GFA of the Zr-Al-Ni-Cu-Lu alloys, characterized by their critical diameters, is not well reflected by the ΔT_x, T_{rg} and γ parameters. Possible explanations have been mentioned in the literature[16, 17].

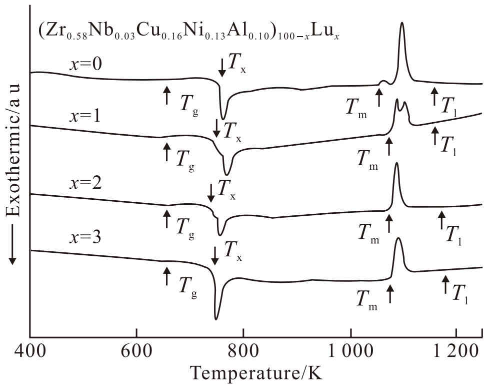

Fig.2 DSC curves of $(Zr_{0.58}Nb_{0.03}Cu_{0.16}Ni_{0.13}Al_{0.10})_{100-x}Lu_x$ (x = 0-3 at%) melt-spun ribbons

It was found that minor addition of rare-earth (RE) elements can significantly improve the GFAs of the BMG-forming alloys[18]. There are three supposed views to explain the beneficial roles of RE elements on the GFAs of glassy alloys. Firstly, RE elements may act as oxygen scavenger via the formation of innocuous RE oxides, leading to the suppression of heterogeneous nucleation[19]. Secondly, there are appropriate atomic-size mismatches, and large negative heat of mixing between the RE elements and the existing constitution elements[20, 21]. Finally, RE elements may destabilize the competing crystalline phase and stabilize the liquid phase[22].

For the glass formation of BMGs, the local atomic structure is crucial. It has been experimentally revealed that a BMG with high GFA generally possesses special atomic configurations that are favorable for improving the GFA[1]. The additional RE elements may promote the formation of special atomic configurations which are favorable for improving the GFA. On the other hand, the local atomic structure of BMGs can reflect the structural features of the initial crystalline phase, which precipitates in the supercooled liquid region during heat treatment[23]. In this paper, we studied the initial crystalline phase of the 2 at% Lu doped alloy as well as the Lu-free alloy. Fig.3 shows the XRD patterns of the annealed $Zr_{58}Nb_3Cu_{16}Ni_{13}Al_{10}$ and $(Zr_{0.58}Nb_{0.03}Cu_{0.16}Ni_{0.13}Al_{0.10})_{98}Lu_2$ samples. Some sharp diffraction peaks are observed in addition to a halo peak corresponding to the residual glassy phase in Figs.3(a) and (b). For the $Zr_{58}Nb_3Cu_{16}Ni_{13}Al_{10}$ glassy alloy, the initial crystalline phases are identified as face-centred-cubic Zr_2Ni (FCC-Zr_2Ni) and tetragonal Zr_2Ni phases. For the $(Zr_{0.58}Nb_{0.03}Cu_{0.16}Ni_{0.13}Al_{0.10})_{98}Lu_2$ glassy alloy, all of the Bragg peaks can be associated with a single icosahedral phase. The indexing of the peaks was carried out on the basis of six independent Millers indices proposed by Bancel *et al*[24]. I-phase precipitation was also confirmed by the nanobeam diffraction patterns with two-, three- and five-fold symmetries for the icosahedral particles. Fig. 4 shows the bright-field TEM image of the $(Zr_{0.58}Nb_{0.03}Cu_{0.16}Ni_{0.13}Al_{0.10})_{98}Lu_2$ ribbons heated to 733 K. The size of the precipitated particles is about 50 nm and their nanobeam diffraction pattern with five-fold symmetry is shown in the inset of Fig.4. For the studied alloys, the final crystalline phases are tetragonal $CuZr_2$ and tetragonal Zr_2Ni, as shown in Figs.3(c) and (d).

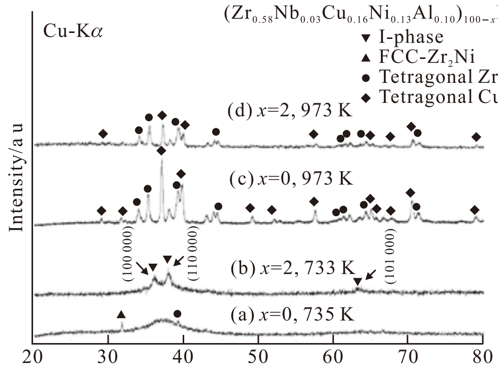

Fig. 3 X-ray diffraction patterns of the melt-spun ribbons heated to different temperatures

The above results indicate that the addition of 2 at% Lu to the Zr-Nb-Cu-Ni-Al alloy induces a change of initial precipitation phases from FCC-Zr_2Ni and tetragonal Zr_2Ni phases for the Lu-free $Zr_{58}Nb_3Cu_{16}Ni_{13}Al_{10}$ alloy to a single I-phase for the Lu-doped alloy, although their final crystalline phases are tetragonal $CuZr_2$ and tetragonal Zr_2Ni. This implies that the local atomic configurations of the $Zr_{58}Nb_3Cu_{16}Ni_{13}Al_{10}$ glassy alloy are changed by Lu addition and the icosahedral-like local structure is the dominant local structure in the Lu-doped glassy alloy. It is suggested that icosahedral clusters exist in the molten Lu-doped alloy and remain in the rapid-solidified glassy alloy, and during annealing the icosahedral clusters arranged to the I-phase, as observed, as a middle phase prior to the final cystallization in our study. The five-fold symmetry of the icosahedral arrangement of atoms is incompatible to the long-ranged translational symmetry, which creates a thermodynamic barrier to the formation of periodic crystals and restrains the crystallization of the molten alloy during rapid solidification, leading to the appearance of superior GFA in the $(Zr_{0.58}Nb_{0.03}Cu_{0.16}Ni_{0.13}Al_{0.10})_{98}Lu_2$ glassy alloy. Accordingly, the existence of strong icosahedral local ordering may be another factor for the higher GFA in the Lu-doped alloys.

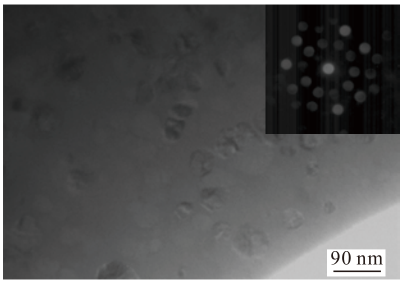

Fig.4 Bright-field TEM image of $(Zr_{0.58}Nb_{0.03}Cu_{0.16}Ni_{0.13}Al_{0.10})_{98}Lu_2$ glassy alloy heated to 733 K (The inset shows the nanobeam diffraction pattern of precipitated I-phase particles with five-fold symmetry)

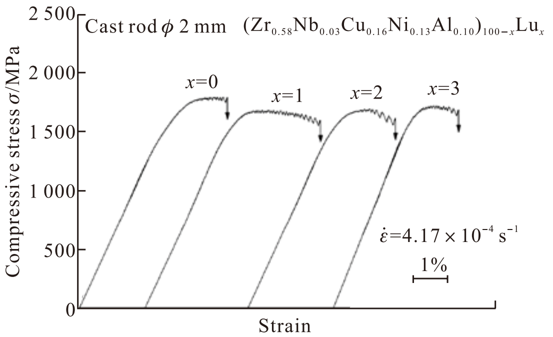

Fig.5 Compressive stress-strain curves of bulk glassy $(Zr_{0.58}Nb_{0.03}Cu_{0.16}Ni_{0.13}Al_{0.10})_{100-x}Lu_x$ (x = 0-3 at%) rods

Fig.5 shows the compressive stress-strain curves of the bulk glassy $(Zr_{0.58}Nb_{0.03}Cu_{0.16}Ni_{0.13}Al_{0.10})_{100-x}Lu_x$ (x = 0 at%, 1 at%, 2 at% and 3 at%) alloy rods with 2 mm in diameter. It can be seen that all the curves exhibit similar features, *i e*, elastic deformation followed by yielding and then distinct plastic deformation accompanying serration prior to failure. The $Zr_{58}Nb_3Cu_{16}Ni_{13}Al_{10}$ glassy alloy exhibits high fracture strength of 1 780 MPa, and slightly detrimental effect of Lu addition can be observed, which is 1 590, 1 610 and 1 680 MPa for $(Zr_{0.58}Nb_{0.03}Cu_{0.16}Ni_{0.13}Al_{0.10})_{100-x}Lu_x$ (x = 1 at%, 2 at% and 3 at%) glassy alloys, respectively. The compressive stress-stain curves also show plastic strain of 1%-2%, indicating the ductile nature of the bulk glassy $(Zr_{0.58}Nb_{0.03}Cu_{0.16}Ni_{0.13}Al_{0.10})_{100-x}Lu_x$ (x = 0 at%, 1 at%, 2 at% and 3 at%) alloys. The plastic strains of the alloys with x=1 at% and 2 at% are higher than the others.

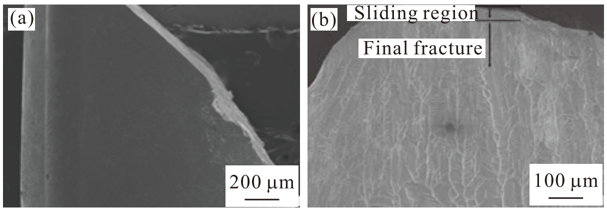

Fig.6 SEM images of compressive fracture of bulk glassy $(Zr_{0.58}Nb_{0.03}Cu_{0.16}Ni_{0.13}Al_{0.10})_{98}Lu_2$ alloy

Fig.6 shows the SEM images of the compressive fracture of the glassy $(Zr_{0.58}Nb_{0.03}Cu_{0.16}Ni_{0.13}Al_{0.10})_{98}Lu_2$ rod. It is observed that samples fracture along a single plane, indicating that one major shear band dominates the final fracture (Fig.6(a)). The compressive fracture angle is approximately 41º, *i e*, smaller than 45º. The fact that the compressive fracture does not occur along the plane of maximum shear stress demonstrates that yielding in the studied BMGs follows the Mohr-Coulomb criterion, rather than the von Mises criterion, which is appropriate to polycrystalline metals. This inclination angle also agrees with those observed during compression of other Zr-based BMGs[25]. The typical fracture morphology in the vicinity of the sample edge is shown in Fig.6(b). In the fracture sliding zone, the surface is relatively smooth except for some thinner ridges and valleys. The feature within the final fracture zone consists of numerous strips and lots of vein patterns. The typical vein-like patterns indicate that a local viscous flow occurs during the fracture process. The good mechanical properties and superior GFA of the Zr-Nb-Cu-Ni-Al-Lu system give it potential applications in industrial fields.

4 Conclusions

Glass-forming ability, thermal stability and mechanical properties of $(Zr_{0.58}Nb_{0.03}Cu_{0.16}Ni_{0.13}Al_{0.10})_{100-x}Lu_x$ (x = 0-3 at%) alloys have been studied. It was found that the GFA of the $Zr_{58}Nb_3Cu_{16}Ni_{13}Al_{10}$

glassy alloy can be greatly enhanced by Lu addition. The critical diameters for glass formation of $(Zr_{0.58}Nb_{0.03}Cu_{0.16}Ni_{0.13}Al_{0.10})_{100-x}Lu_x$ (x = 1 at%, 2 at% and 3 at%) alloys are 15, 20 and 12 mm, respectively, while that of the Lu-free $Zr_{58}Nb_3Cu_{16}Ni_{13}Al_{10}$ alloy is only 7 mm. The ΔT_x value decreases from 92 to 79 K with the Lu content increasing from 0 to 2 at%, and then increases to 91 K at 3 at% Lu. The change of initial precipitated crystalline phase from the FCC-Zr_2Ni and tetragonal Zr_2Ni phases to a single I-phase by the addition of Lu may be correlated to the improvement of GFA of the Lu-doped alloys. The fracture strength of the bulk glassy $(Zr_{0.58}Nb_{0.03}Cu_{0.16}Ni_{0.13}Al_{0.10})_{100-x}Lu_x$ (x = 0 at%, 1 at%, 2 at% and 3 at%) alloys is 1 780, 1 590, 1 610 and 1 680 MPa, respectively, and the compressive plastic strain of the studied alloys is over 1%.

References

[1] Inoue A and Takeuchi A. Recent Progress in Bulk Glassy Alloys[J]. *Mater. Trans. JIM*, 2002, 43(8): 1 892-1 906

[2] Johnson W L. Bulk Glass-forming Metallic Alloys: Science and Technology[J]. *Mater. Res. Bull.*, 1999, 24(10): 42-56

[3] Tao P J, Yang Y Z, Guan G J, *et al.* Effect of Heat Treatment on the Mechanical Properties of FeCoZrWB Bulk Metallic Glass[J]. *J. Wuhan Univ. Technol. -Mater. Sci. Ed.*, 2012, 27(3): 547-549

[4] Zhang T, Inoue A and Masumoto T. Amorphous Zr-Al-Tm (Tm = Co, Ni, Cu) Alloys with Significant Supercooled Liquid Region of Over 100 K[J]. *Mater. Trans. JIM*, 1991, 32(11): 1 005-1 010

[5] Peker A and Johnson W L. A Highly Processable Metallic Glass: $Zr_{41.2}Ti_{13.8}Cu_{12.5}Ni_{10.0}Be_{22.5}$[J]. *Appl. Phys. Lett.*, 1993, 63 (17): 2 342-2 344

[6] Wang Y, Shi L L, Duan D L *et al*. Tribological Properties of $Zr_{61}Ti_2Cu_{25}Al_{12}$ Bulk Metallic Glass under Simulated Physiological Conditions[J]. *Mater. Sci. Eng. C*, 2012, 37(3): 292-304

[7] Peter W H, Buchanan R A, Liu C T, *et al*. Localized Corrosion Behavior of a Zirconium-based Bulk Metallic Glass Relative to Its Crystalline State[J]. *Intermetallics*, 2002, 10(11-12): 1 157-1 162

[8] Inoue A and Takeuchi A. Recent Progress in Bulk Glassy, Nanoquasicrystalline and Nanocrystallic Alloys[J]. *Mater. Sci. Eng. A*, 2004, 375-377: 16-30

[9] Inoue A, Zhang T, Nishiyama N, *et al.* Preparation of 16 mm Diameter Rod of Amorphous $Zr_{65}Al_{7.5}Ni_{10}Cu_{17.5}$ Alloy[J]. *Mater. Trans., JIM*, 1993, 34(12): 1 234-1 237

[10] Hays C C, Schroers J, Geyer U, *et al.* Glass Forming Ability in the Zr-Nb-Ni-Cu-Al Bulk Metallic Glasses[J]. *Mater. Sci. Forum*, 2000, 343-346: 103-108

[11] Lin X H, Johnson W L and Rhim W K. Effect of Oxygen Impurity on Crystallization of an Undercooled Bulk Glass Forming Zr-Ti-Cu-Ni-Al Alloy[J]. *Mater. Trans. JIM*, 1997, 38(5): 474-477

[12] Jiang Q K, Wang X D, Nie X P, *et al.* Zr-(Cu, Ag)-Al Bulk Metallic Glasses[J]. *Acta Mater*., 2008, 56 (8): 1 785-1 796

[13] Hua N B, Pang S J, Li Y, *et al.* Ni- and Cu-free Zr–Al–Co–Ag Bulk Metallic Glasses with Superior Glass-forming Ability[J]. *J. Mater. Res.*, 2011, 26(4): 539-546

[14] Zhao X J, Ma C L, Pang S J, *et al.*The Glass-forming Ability and the I-phase Formation in Y-doped Zr-Nb-Cu-Ni-Al Glassy Alloys[J]. *Philos. Mag. Lett*., 2009, 89(1): 11-18

[15] Lu Z P and Liu C T. A New Glass-forming Ability Criterion for Bulk Metallic Glasses[J]. *Acta Mater*., 2002, 50(13): 3 501-3 512

[16] Tan H, Zhang Y, Ma D, *et al.* Optimum Glass Formation at Off-eutectic Composition and Its Relation to Skewed Eutectic Coupled Zone in the La based La-Al-(Cu,Ni) Pseudo Ternary System[J]. *Acta Mater*., 2003, 51(15): 4 551-4 561

[17] Ma D, Tan H, Wang D, *et al.* Strategy for Pinpointing the Best Glass-forming Alloys[J]. *Appl. Phys. Lett.*, 2005, 86(19):191 906-3

[18] Wang W H. Roles of Minor Additions in Formation and Properties of Bulk Metallic Glasses[J]. *Prog. Mater. Sci*., 2007, 52 (4): 540-596

[19] Zhang Y, Pan M X, Zhao D Q, *et al*. Formation of Zr-based Bulk Metallic Glasses from Low Purity of Materials by Yittrium Additon[J]. *Mater. Trans. JIM*, 2000, 41(11): 1 410-1 414

[20] Xu D H, Duan G, and Johnson W L. Unusual Glass-forming Ability of Bulk Amorphous Alloys based on Ordinary Metal Copper[J]. *Phys. Rev. Lett.*, 2004, 92 (24): 245 504-4

[21] Lu Z P, Liu C T, and Porter W D. Role of Yttrium in Glass Formation of Fe-based Bulk Metallic Glasses[J]. *Appl. Phys. Lett*., 2003, 83(13): 2 581-2 583

[22] Mihalkovic M and Widom M. *Ab Initio* Calculations of Cohesive Energies of Fe-based Glass-forming Alloys[J]. *Phys. Rev. B*, 2004, 70(14):144 107-144 112

[23] Wang W H, Dong C and Shek C H. Bulk Metallic Glasses[J]. *Mater. Sci. Eng. R*, 2004, 44 (2-3): 45-89

[24] Bancel P A, Heiney P A, Stephens P W, *et al.* Structure of Rapidly Quenched Al-Mn[J]. *Phys. Rev. Lett*., 1985, 54(22): 2 422-2 425

[25] Wright W L, Saha R and Nix W D. Deformation Mechanisms of the $Zr_{40}Ti_{14}Ni_{10}Cu_{12}Be_{24}$ Bulk Metallic Glass[J]. *Mater. Trans. JIM*, 2001, 42(4):642-649